

## On robots and flies: Modeling the visual orientation behavior of flies

Susanne A. Huber\*, Matthias O. Franz, Heinrich H. Bülthoff

Max Planck Institute für Biological Cybernetics, Spemannstr. 38, 72076 Tübingen, Germany

Received 16 February 1998; received in revised form 20 July 1998

Communicated by F.C.A. Groen

### Abstract

Although artificial and biological systems face similar sensorimotor control problems, until today only a few attempts have been made to implement specific biological control structures on robots. Nevertheless, the process of designing the sensorimotor control of a robot can contribute to our understanding of these mechanisms and can provide the basis of a critical evaluation of existing biological models. Flies have developed a specialized visuomotor control for tasks such as course stabilization, fixation and approach towards stationary objects, tracking of moving objects and landing, which are based on the analysis of visual motion information. Theoretical and experimental results suggest that in flies the visuomotor control for course stabilization as well as fixation and approach towards stationary objects may be implemented at least partially by one common sensory circuit. We present agents with a visuomotor controller that regulates the two behaviors of course stabilization and object fixation. To test this controller under real world conditions, we implemented it on a miniature robot. We have been able to show that in addition to course stabilization and object fixation, the robot also approaches stationary objects. ©1999 Elsevier Science B.V. All rights reserved.

*Keywords:* Visual information processing; Sensorimotor control; Fly behavior; Object fixation; Autonomous agents

### 1. Introduction

#### 1.1. Biology for robotics

In many aspects of technological applications an increasingly important goal is to build robust autonomous robots that are able to achieve tasks in a dynamic and unpredictable environment. Robots are particularly needed where humans are not able to survive and remote control is difficult to implement (e.g., repair of sewage systems, expedition to Mars,

volcanoes or deep sea explorations). By studying natural systems, much can be learnt about the design of technical solutions.

Recently, behavioral mechanisms of biological systems have specifically been considered more closely for the design of autonomous mobile robots. The suggestion of Tinbergen [46] on behavioral modules for the description of complex behavior in biological systems has turned out to serve as a good model for robust control of behavior in autonomous robots. Evolutionary, developmental and learning processes have been applied to adaptive control of autonomous agents [17,26]. In addition, several researchers have stressed that the environment plays an important role in the adequate organization of behavior and thereby reduces the complexity of internal mechanisms [3,4].

\* Corresponding author. Present address: University of Zurich, Institute of Psychology, Attenhoferstr. 9, CH-8032 Zurich, Switzerland. Tel.: +1-634-21-38; fax: +1-634-49-29  
E-mail address: shuber@genpsy.unizh.ch (S.A. Huber)

Until today, however, these concepts have been applied to the field of robotics only on a very abstract level and many problems still remain unsolved. Models of biological systems have been used for robot control and actual sensorimotor mechanisms of biological systems have been implemented into robots (e.g., [2,8,11,50]), although little is known about the functionality of many sensorimotor processes in biological systems. Autonomous robots and simulated agents, e.g., have been designed with orientation mechanisms that are inspired by the behavior of flies. Visuomotor controllers have been developed that use visual motion information. Mostly these agents use the visual motion information for obstacle avoidance [12,18,51] or tracking of other objects [8,35].

### 1.2. Robots for biology

The development of robots that are inspired by living organisms does not only have a major influence on the development of new technologies but is also a promising complementary research approach for the study of biological systems. The simulation of simple life forms and the implementation of behavioral models on robots may be especially useful to our understanding of biological systems, e.g., to test models of biological information processing.

Information processing has been studied in insects for many years because insects show stimulus–response characteristics that allow insight into the mechanisms of visual processing as well as into the interaction of sensory input and motor output. Especially the visually controlled orientation behavior of flies is particularly well studied under controlled conditions with walking or tethered flying flies [21,24,31,42] as well as in free flight situations [6,10,33,48,52].

Results from fly research suggest that the two behaviors of course stabilization and approach towards stationary objects may be realized at least partially by one common behavioral module [5,9,23,24,42]. Reichardt and Poggio [42] used differential equations to describe these orientation behaviors of flies. In our work, we use the robotics approach to investigate this hypothesis. Our goal is to build a single visuomotor controller that regulates both behaviors. We modeled the subsequent processing steps in the

visual system of flies in detail. Like the robots of Franceschini et al. [18] and others, the agent uses visual motion information of a 360° horizontal field of view for behavior control. We can demonstrate that our computer-simulated agent is able to control the two behaviors of course stabilization and approach towards stationary objects by evaluating the motion information with a single visuomotor controller. To test the behaviors under real world conditions, we implement the control structure on a miniature robot – the *Khepera*<sup>TM</sup> [36].

## 2. Visuomotor control of a computer-simulated agent

### 2.1. Model of the visual system

The large compound eyes of the fruitfly *Drosophila melanogaster* each consist of about 700 ommatidia. The visual signals on the retinae are processed in three neural layers: the neuropils lamina (L), medulla (M) and lobula complex which again can be divided into the anterior lobula (LO) and the posterior lobula plate (LP) (Fig. 1).

Results on fly research suggest that the neurons in these layers are responsible for contrast enhancement, reduction of signal redundancy, signal amplification, motion detection and evaluation of the motion signals [21,27,28,45]. We have implemented these levels of visual information processing in a simplified model (Fig. 2).

#### 2.1.1. Spatial lowpass filtering in the retina

The agent had a horizontal array of sensors with a 360° field of view which scanned the visual world at the horizon. The visual input to the sensors was spatially lowpass filtered by Gaussian filters ( $\sigma = 3.8^\circ$ ). As in *Drosophila* [21], the optical axes of the sensors had an angular distance of  $d\varphi = 4.6^\circ$ . Hence the array had 78 sensors.

#### 2.1.2. Redundancy reduction and amplification of the signal in the lamina

In flies large monopolar cells (LMCs) in the lamina are known to be responsible for local contrast enhancement both by reducing redundant parts of the signal and by signal amplification [34,45]. We have modeled

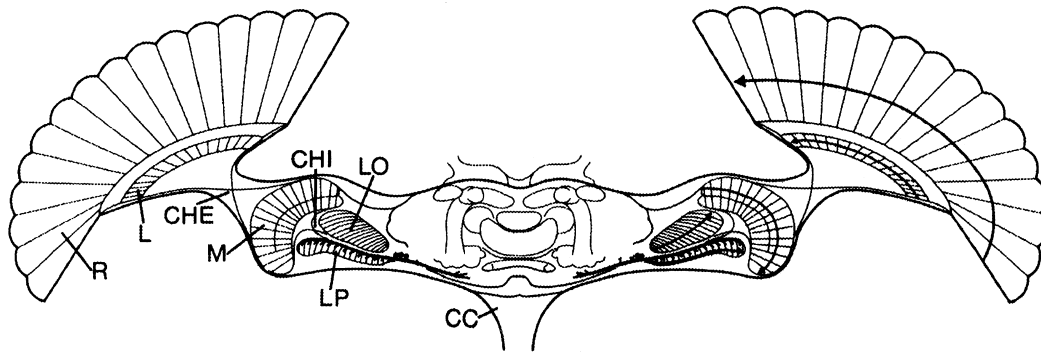


Fig. 1. Cross-section through the fly's brain with large compound eyes (redrawn from [28]), the retina (R), lamina (L), medulla (M), lobula (LO), lobula plate (LP) and the cervical connective (CC). The lamina and medulla are connected via the external chiasm (CHE) and the medulla and lobula complex via the internal chiasm (CHI).

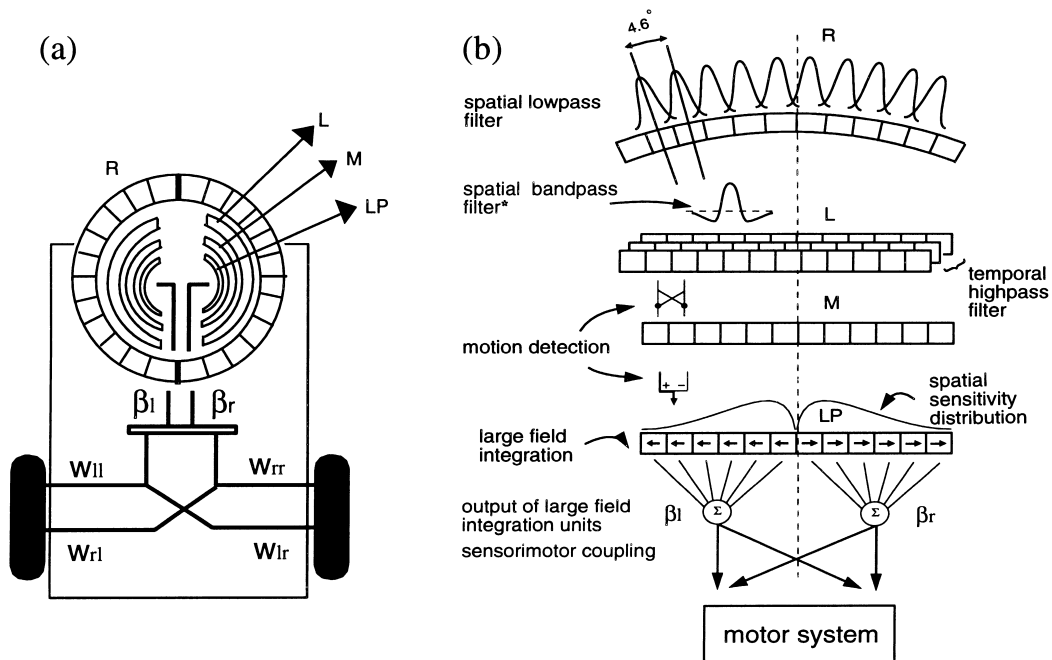


Fig. 2. Sketch of the agent with ring sensor (R), simplified models of the three layers of the visual system: lamina (L), medulla (M), lobula plate (LP), and the transmission weights ( $w_l$ ,  $w_r$ ,  $w_{rl}$ ,  $w_{rr}$ ) that couple the outputs of the large field units ( $\beta_l$ ,  $\beta_r$ ) to the motor system. (b) Model of the visuomotor controller with the functional processing steps that take place in the different layers of the agent's visual system ((\* the bandpass filter is only realized on the *Khepera*<sup>TM</sup> robot, see Section 4).

the temporal aspects of the LMC cells by applying a temporal highpass filter  $H$  ( $\tau_H = 20.0$  steps, where one step corresponds to one simulation cycle), which eliminates temporally redundant parts of the signal, i.e. signals which are steady or slowly changing in time. The signals are then linearly amplified to the full range of 256 gray-level values.

### 2.1.3. Motion detection and evaluation in the medulla and lobula plate

Compared to human eyes the resolution of the compound eyes is very coarse. Thus, the perception of shape is more difficult. There is strong evidence that for visual orientation the detection of motion plays a prominent role (e.g., [27,40]). For motion percep-

tion in insects, Hassenstein and Reichardt [27] proposed a detector which correlates temporal modulation of image intensities in two neighboring ommatidia. The detector model has two mirror-symmetrical subunits. In each subunit the signals of two input channels are multiplied after the signals have been filtered by two lowpass filters with different time constants. We have modeled the lowpass filters of the motion detectors with the time constants  $\tau_1 = 1.5$  steps and  $\tau_2 = 5.0$  steps. The outputs of the two subunits are then subtracted to obtain the direction of the motion stimulus. From electrophysiological studies it has been concluded that the subtraction stage of the movement detector is localized on the dendrites of the large field tangential neurons within the lobula plate of the fly (review: [29]).

These neurons integrate the motion signals over large receptive fields, and are specialized in terms of certain motion patterns. For example, the horizontal equatorial cells (HSE cells) respond maximally to horizontal progressive motion in the frontolateral field of view. The HSE cells receive input from motion detectors that respond more strongly to a pattern moving horizontally from front to back (progressive motion) than from back to front (regressive motion). The asymmetry results from the fact that the time course of these motion detector subunits is not completely mirror symmetric [16]. The asymmetric response of the detector subunits is modeled by a gain of 1.0 for progressive and 0.7 for regressive motion.

Modeling the HSE cells, two large field units integrate the motion information over a  $184^\circ$  field of view in the right and left hemisphere with an overlapping region of  $8^\circ$  in the front. The sensitivity distribution  $S(j)$  ( $j$  number of sensors, where the sensors  $\pm 1$  are oriented at the visual angles  $\varphi = \pm 2.3^\circ$  off the heading direction and the sensors  $\pm 39$  at  $\varphi = \pm 177.1^\circ$ ) is modeled by the function:

$$S(j) = aj^b e^{-cj} \quad (1)$$

with  $a = 0.625$ ,  $b = 0.7$  and  $c = 0.15$  and  $j \in [-1, 39]$  (see also Fig. 3).  $S(j)$  is bilaterally symmetrical for the two integration units ( $S(j) = S(-j)$ ) and the maximum of  $S(j)$  is at the sensor 5 (at  $\varphi_{\max} = 23^\circ$ ). The outputs ( $\beta_1, \beta_r$ ) of the integration units are coupled via transmission weights to the motor system.

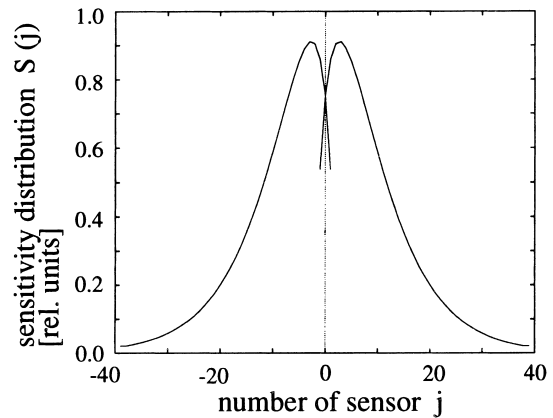


Fig. 3. The spatial sensitivity distribution of both large field units.

## 2.2. Model of the motor system

The agent was modeled as a simple kinematic system with two motors, ignoring its mass and inertia. This approximation can be made in the modeling of the visuomotor control of flies, because after an initial acceleration, within a short time ( $< 10$  ms) the fly reaches a constant velocity as the force produced by the wings is balanced by the increasing air friction. The motors had a distance of  $c = 1$  u, given in units u of the agent's widths ( $1 \text{ u} = 0.25 \text{ cm}$ ). The force vectors produced by the wings of the fruitfly *Drosophila* have an estimated perpendicular distance from the center of the fly of about 0.2–0.3 cm (body-length: 0.3 cm) [21].

The velocities  $\mathbf{v}_l = (0, v_l)$  and  $\mathbf{v}_r = (0, v_r)$  (Fig. 4) of the motors were proportional to the force of the two motors. Each motor produced a constant velocity  $v_0 = 0.1 \text{ u/step}$  which was modulated by the outputs of the processed visual information:

$$v_l = v_0 - T(s_l), \quad v_r = v_0 - T(s_r). \quad (2)$$

The signals  $s_l$  and  $s_r$  result from the visual motion information via the control signals  $m_l$  and  $m_r$  and intrinsic noise  $n_l$  and  $n_r$  (Fig. 5):

$$s_l = km_l + n_l, \quad s_r = km_r + n_r, \quad (3)$$

where  $k$  is a proportionality factor. The control signals  $m_l$  and  $m_r$  are explained in detail in Section 2.3.

As the force produced by the wings of the fly never becomes negative, the velocities  $v_l$  and  $v_r$  are always greater than or equal to  $0 \text{ u/step}$ . This was achieved by

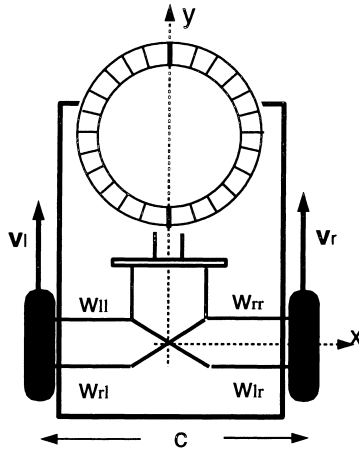


Fig. 4. Motor system of the simulated agent. The motors are separated by a distance  $c$  and lead to velocities  $v_l$  and  $v_r$ .

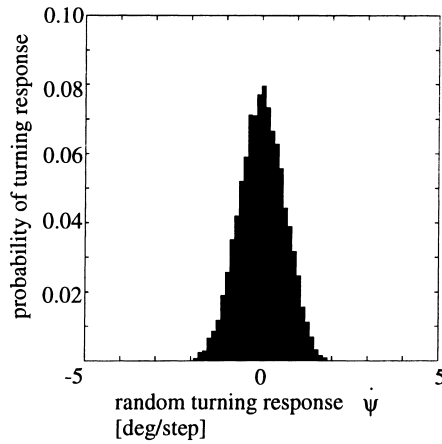


Fig. 5. Noise signal  $n_l$  of left motor (Gaussian distribution with  $\sigma = 0.64^\circ/\text{step}$ ).

the sigmoid function  $T(s)$  for the left and right motor, respectively:

$$T(s) = \begin{cases} -v_0 & \text{if } s < -v_0, \\ s & \text{if } |s| \leq v_0, \\ v_0 & \text{if } s > v_0. \end{cases} \quad (4)$$

The system had two degrees of freedom: translation in the heading direction and rotation around the vertical body-axis. The translatory and rotatory velocities were

$$v_t = \frac{v_r + v_l}{2} \quad \text{and} \quad \dot{\psi} = \frac{v_r - v_l}{c}. \quad (5)$$

### 2.3. Coupling of sensor and motor systems

#### 2.3.1. Orientation towards stationary objects

In behavioral studies with flies, Reichardt and Poggio [38,42] showed that the fly orients itself towards a single black stripe in an otherwise homogeneous arena. This so-called fixation behavior is in contrast to a fly's behavior in a visually homogeneous environment, where it turns in all directions with equal probability. Due to intrinsic noise the motor system continuously produces torque, resulting in turning movements in either direction. The noise has a Gaussian distribution [42].

One explanation of the fixation behavior is based on the fact that the turning response of flies in open-loop experiments is stronger if a stripe moves from front to back than in the other direction [31] due to the asymmetric response of the HS-neurons. As the noisy torque signals of the motor system lead to movements of an object's retinal image, the resulting image flow will cause the fly to orient towards the object because the positive response to progressive motion is stronger than the negative response to regressive motion.

Besides the large field cells also the small field cells [13–15,28,30] are assumed to participate in object fixation and additionally in tracking moving objects. These cells respond selectively to motion in small areas of their receptive field. As these cells have not been included into our model controller, we will not describe them in further detail here.

In experiments where two stripes (at various angular separations  $\Delta\psi_s$ , up to  $180^\circ$ ) are presented, the fly does not show any preference for either one of the stripes. For a separation of the stripes of  $\Delta\psi_s < 40^\circ$ , flies fixate at the middle point between the two stripes. At around  $\Delta\psi_s = 40^\circ$ – $60^\circ$ , there is a transition from one stable orientation to two stable orientations. For  $\Delta\psi_s \geq 60^\circ$ , flies fixate on one stripe for a certain amount of time, then switch to the second stripe, fixate and switch back etc. They fixate upon each stripe for approximately the same amount of time. Flies, however, do not fixate directly on the center of each stripe but fixate a point off the center such that the fly is slightly oriented towards the other stripe. Especially for  $\psi_s = 60^\circ$ , there is a high variation of the fixation behavior of individual flies and the fixation point lies between about  $2^\circ$  and  $15^\circ$  off the center of the stripe. No such scatter was observed for  $\Delta\psi_s = 80^\circ$ – $180^\circ$ .

At an angular separation of  $180^\circ$  an almost exact fixation on the center of the stripe has been observed [38,41,42].

To test the model of the fixation behavior of flies, the signals that result from the large field integration units were coupled proportionally to the motor system.

$$\begin{aligned} m_1^f(t) &= \omega_{ll}\beta_l + \omega_{lr}\beta_r, \\ m_r^f(t) &= \omega_{rl}\beta_l + \omega_{rr}\beta_r. \end{aligned} \quad (6)$$

The matrix

$$\mathbf{W} = \begin{pmatrix} \omega_{ll} & \omega_{lr} \\ \omega_{rl} & \omega_{rr} \end{pmatrix} = \begin{pmatrix} 0.9 & -0.4 \\ -0.4 & 0.9 \end{pmatrix} \quad (7)$$

contains the transmission weights for the coupling of the outputs  $\beta_l$  and  $\beta_r$  of the two large field integration units to the left and right motor. We assumed bilateral symmetry for the sensorimotor coupling.

### 2.3.2. Optomotor response

While flying, flies are continuously stabilizing their course. In order to compensate for disturbances, which cause large rotatory image motion, they execute turning movements — the so-called optomotor response — along the direction of the image motion. This behavior may be implemented by cells that integrate the difference of the output signals from the horizontal cells in the two optic lobes [31,43]. A motor signal, simply proportional to the difference of the image motion in the two eyes, has two major disadvantages:

1. The response of the Reichardt motion detector increases with increasing image motion up to an optimum and decreases again for faster motion. Due to this response characteristic, ambiguous response signals result with respect to pattern velocity. It is impossible to decide from the visual signal alone whether the image motion resulted from a pattern that moves at low or very high speed. Full compensation is not possible.
2. In general, a purely proportional controller (without memory) may cause oscillations because the compensation behavior is active only until the retinal image is stabilized. As the disturbance persists, image flow will again be detected and the compensation behavior is once more active until the retinal image is stabilized again, etc.

This second point, however, does not seem to be a disadvantage for the control system of flies. Warzecha and Egelhaaf [49] could show that, due to the response characteristic of the motion detector, large-amplitude fluctuations in the image motion, generated when the optomotor system becomes unstable, are transmitted with a small gain; this leads to only relatively small turning responses and thus small image motion.

To model the optomotor response behavior, the signals  $\beta_l$  and  $\beta_r$  that result from the large field units were integrated over time. The realization of this stage in biological systems is most probably different from a pure, linear integration [43], but are not modeled in more detail here.

In simulation the integration was replaced by a summation:

$$B_l(t) = \sum_{-\infty}^t \beta_l(t'), \quad B_r(t) = \sum_{-\infty}^t \beta_r(t'). \quad (8)$$

The coupling of these signals to the motor system leads to the control signals:

$$\begin{aligned} m_1^{or}(t) &= \omega_{ll}B_l(t) + \omega_{lr}B_r(t), \\ m_r^{or}(t) &= \omega_{rl}B_l(t) + \omega_{rr}B_r(t), \end{aligned} \quad (9)$$

with the transmission weights from Eq. (7).

### 2.3.3. Optomotor response and object fixation

Experimental results suggest that the behaviors for course stabilization and approach towards stationary objects of flies may be implemented at least partially by a common sensory circuit [5,23,24,42]. In order to test this we designed agents with a visuomotor controller that regulated both the optomotor response and the fixation behavior. For the controller the control signals for optomotor response  $m_{or}$  and object fixation  $m_f$  were combined into a proportional-integral controller:

$$\begin{aligned} m_l(t) &= k_f m_1^f(t) + k_{or} m_1^{or}(t), \\ m_r(t) &= k_f m_r^f(t) + k_{or} m_r^{or}(t), \end{aligned} \quad (10)$$

with the constant factors  $k_f = 0.5$  u/step and  $k_{or} = 5.0 \cdot 10^{-4}$  u/step. A similar processing step is used in computer simulations to model the figure-ground discrimination in the visual system of flies [43] and has also been described to explain data of the oculomotor signals in primates, where a pulse of activity is transformed into a sum of the pulse and its integral before being transferred to the motor neurons [7].

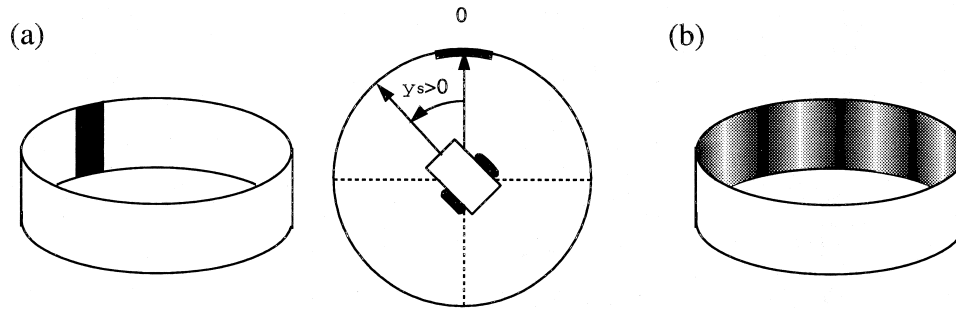


Fig. 6. Sketch of simulated arena: (a) side view of the arena with a sinusoidal pattern and (b) with one black stripe, and (c) top view. The stripe is at  $0^\circ$ , initial orientation of agent is at  $\psi_s$ .

### 3. Experiments with the simulated agent

#### 3.1. Fixation behavior

To compare the performance of the fixation behavior of the agent with that of flies in the studies of Reichardt and Poggio [38,39,42], we ran three experiments. In all three, the agent was fixed in the middle of a drum and therefore had only one degree of freedom, the rotation around its vertical body axis. The angular velocity of the turning response  $\dot{\psi}$  is given by Eq. (5).

**Experiment 1 (Fixation on a single stripe).** A single black stripe (angular width  $17.3^\circ$ ) was presented on the wall of the drum in an otherwise white surrounding (Fig. 6(a) and (b)). The initial orientation of the agent was  $\psi_s = 41.4^\circ$ . The simulation ran for 10 000 time steps.

**Result.** Due to torque fluctuations caused by intrinsic noise of the system, the retinal image of the stripe was not stationary. The agent turned towards the object because the turning response was stronger to progressive than to regressive motion. Within 1100 steps the agent oriented towards the stripe. For the rest of the simulation the agent was able to fixate on the stripe (Fig. 7). The slightly overlapping receptive fields of the integration units were necessary for the agent to keep the stripe in the front because agents which lack this characteristic were not able to fixate on the stripe in front of them.

**Experiment 2 (Fixation on two stripes).** In this experiment we ran five simulations with two black stripes (angular width  $17.3^\circ$  each) at an angular

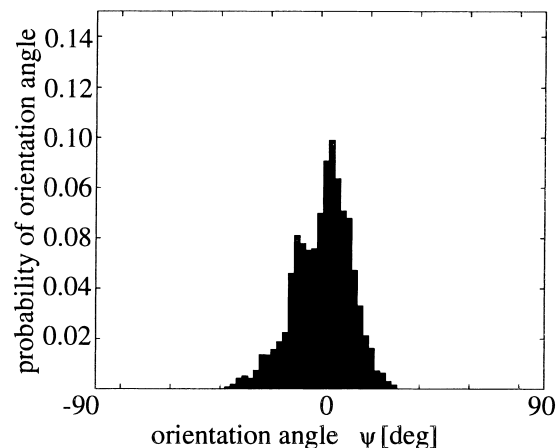


Fig. 7. Histogram of the agent's orientation angle  $\psi$  in a drum with one stripe at  $\psi_s = 0.0^\circ$ :  $\bar{\psi} = 0.95^\circ \pm 11.21^\circ$ .

separation of  $\Delta\psi_s = 40^\circ, 60^\circ, 80^\circ, 100^\circ$ , or  $180^\circ$ , respectively, on the otherwise white wall of the drum. In order to simulate the fixation behavior for two stripes, the agent was turned away from one stripe after every 2000 time steps by a large rotation angle of  $|\psi| = 72^\circ$  for  $\Delta\psi_s < 180^\circ$  and of  $|\psi| = 144.0^\circ$  for  $\Delta\psi_s = 180^\circ$ . The direction of the rotation was chosen randomly. The simulations ran for 50 000 steps each.

**Result.** Similar to the experiments with flies a transition from one stable orientation to two stable orientations took place. At an angular separation of the two stripes of  $\Delta\psi_s = 40^\circ$  the histogram shows a single peak in the middle between the two stripes (Fig. 8). For  $\Delta\psi_s > 40^\circ$  the agent either fixated on one or the other stripe. The influence of the sensitivity function

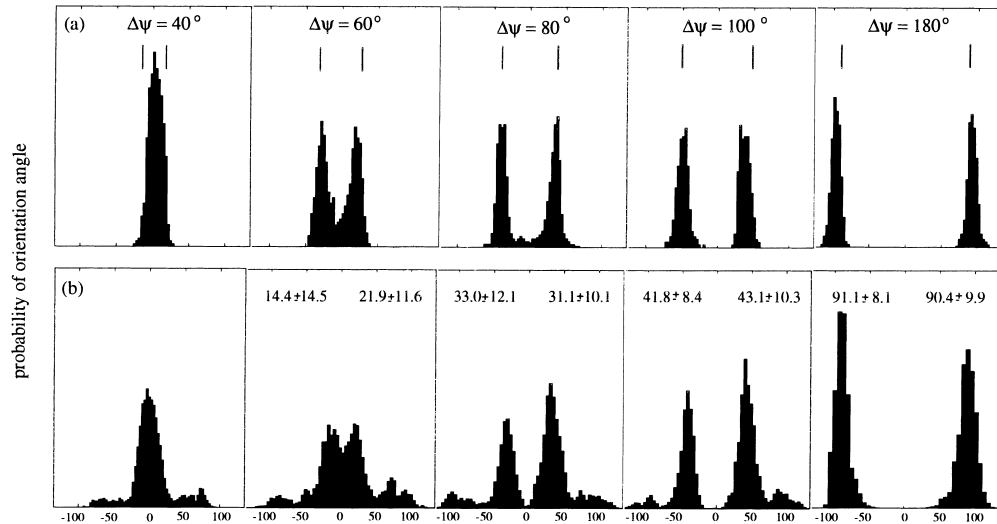


Fig. 8. (a) Fixation behavior of a fly for two stripes (redrawn from [42]) with angular separation of  $\Delta\psi_s = 40^\circ, 60^\circ, 80^\circ, 100^\circ$ , and  $180^\circ$ . Histogram of the error angle  $\psi$  between the heading direction of the fly and the stripes in the drum. (b) Fixation behavior of a simulated agent. Histogram of the agent's orientation angle  $\psi$  in a drum. Angles of the peak and standard deviations of the bimodal Gaussian distribution are given in the diagram.

of the large field integration units is essential for this behavior. When agents were tested with a uniform sensitivity distribution, they fixated for all  $\Delta\psi_s$  on a point in the middle between the stripes, where the contrast distribution and thus the image motion on the left and right eye are equal. Yet, with the sensitivity distribution  $S(j)$  (Eq. (1)), the optical flow resulting from the stripe nearest to the heading direction had a higher influence on the turning response; the agent thus fixated on that stripe.

For  $\Delta\psi_s = 60^\circ, 80^\circ$  and  $100^\circ$ , the bimodal histogram<sup>1</sup> of the orientation angles shows that the agent did not fixate directly on the center of the stripe because the estimated angular separation of the peaks of the histogram (Fig. 8) is smaller than the angular separation of the two stripes. For  $\Delta\psi_s = 180^\circ$  the agent directly fixated on the center of the stripes.

**Experiment 3** (*Fixation on a stripe on a textured surrounding pattern*). On the walls of the drum a stripe (contrast  $C = 1.0$ ) was presented with a surrounding sinusoidal pattern ( $C = 0.5$  and  $\lambda = 36^\circ$ ). The start-

ing orientation of the agent was at  $\psi_s = 61.8^\circ$ . The simulation ran for 10 000 steps.

**Result.** The agent fixated on this stripe after 1300 steps, although due to its own turning response the motion signal that resulted from the sinusoidal pattern was non-zero (Fig. 9). Due to the contrast dependency of the motion detectors, the signal that resulted from

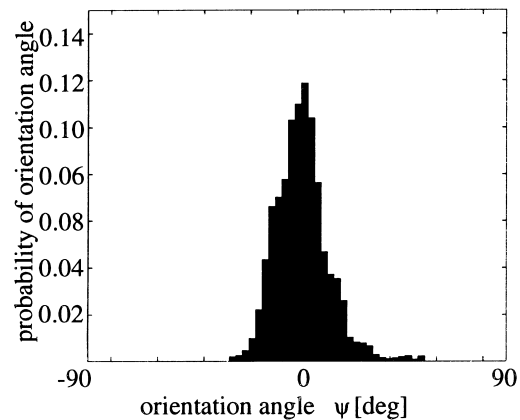


Fig. 9. Histogram of the agent's orientation angle  $\psi$  in a drum with sinusoidal pattern of low contrast and one prominent stripe (at  $\psi_s = 0.0^\circ$ ):  $\psi = 1.99^\circ \pm 11.24^\circ$ .

<sup>1</sup> To obtain the maxima and variance of the bimodal histogram (Fig. 8) of orientation angles, the sum of two Gaussian distributions is fitted to the data.

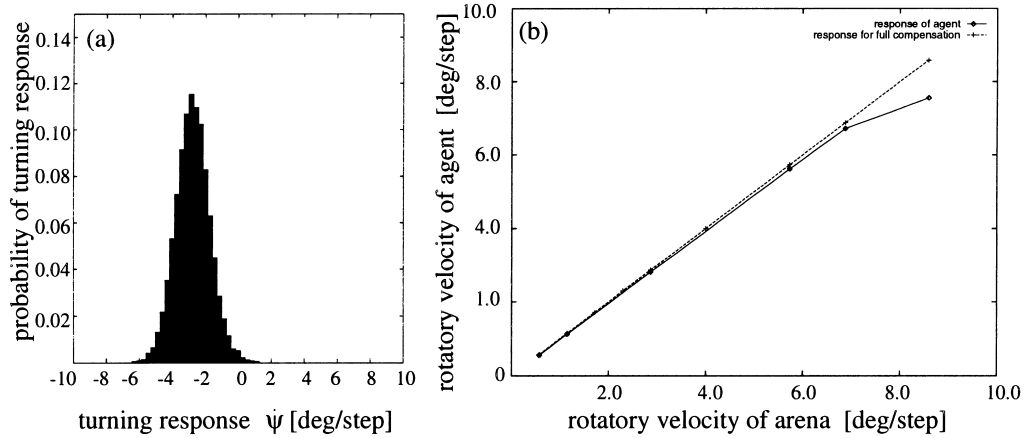


Fig. 10. Optomotor response. (a) Histogram of the agent's optomotor response. The agent is fixed at the center of a rotating drum. Rotation of drum:  $\dot{\psi}_d = 2.9^\circ/\text{step}$ ; rotation of agent:  $\dot{\psi} = 2.8 \pm 1.0^\circ/\text{step}$ . (b) The agent's optomotor response is dependent on the angular speed of the arena.

the prominent stripe was much larger than that from the sinusoidal pattern, resulting in a turning response towards the stripe.

### 3.2. Optomotor response behavior

**Experiment 4.** As in the previous experiment, the agent was fixed in the middle of a drum and could only turn around its vertical body axis. In order to test the optomotor response a sinusoidal pattern ( $\lambda = 36^\circ$ ) (Fig. 6(c)) rotated with a constant angular velocity  $\dot{\psi}_d$ . The simulations ran for 10 000 time steps with different velocities  $\dot{\psi}_d$  (Fig. 10(b)).

**Result.** In order to stabilize the retinal image and thus its orientation in the drum, the agent produced on an average a compensatory turning response of  $\bar{\dot{\psi}} \pm \sigma_{\dot{\psi}}$  (Fig. 10). The agent was able to compensate for 97% of the arena's rotation when the angular velocity was lower than  $7^\circ/\text{step}$ . Due to the sigmoid function (Eq. (4)) the agent was not able to compensate to this extent for higher velocities of the drum.

**Experiment 5.** As Warzecha and Egelhaaf [39,49] suggested a simple proportional controller for the generation of the optomotor response behavior, we also tested the performance of the agent with a proportional controller:

$$m_l(t) = k_f m_l^f(t), \quad m_r(t) = k_f m_r^f(t), \quad (11)$$

with the constant factors  $k_f = 0.5$  u/step.

**Result.** With a purely proportional controller the agent was able to compensate for only 35% of the external rotation of the drum ( $\bar{\dot{\psi}} = 1.0 \pm 1.3^\circ/\text{step}$ ). However, the standard deviation was only slightly larger than with the proportional-integral controller.

## 4. Implementation on the robot

The controller was implemented on a mobile robot, the *Khepera*<sup>TM</sup> (Fig. 11). The imaging system on the robot consists of a conical mirror mounted above a small video camera. The optical axis of the video camera is oriented to the center of the cone. This configuration provides a  $360^\circ$  horizontal field of view extending from  $10^\circ$  below to  $10^\circ$  above the horizon [19]. The image was sampled on five circles along the horizon within a vertical aperture of  $2.1^\circ$ . The samples were averaged vertically to provide robustness against inaccuracies in the imaging system. Then the samples were horizontally lowpass filtered using a Gaussian filter, resulting in 96 sensors on the horizontal ring, 48 for each eye. The resolution was higher than in the simulation.

In processing of the video images, we modelled both the temporal aspects of the LMCs and their spatial aspects, the latter by using a spatial band-pass filter obtained by predictive coding — a procedure known as image compression (e.g., [53]).

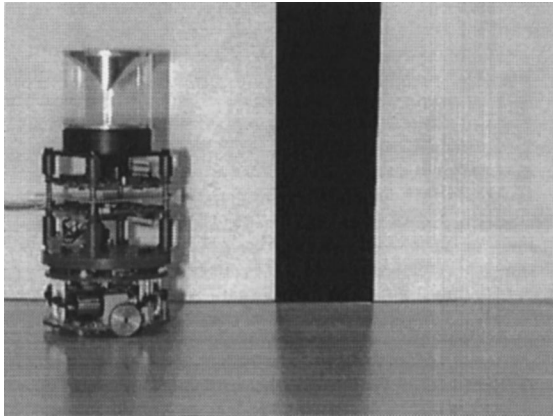


Fig. 11. *Khepera*<sup>TM</sup> robot with vision module. The optical axis of the camera is oriented vertically upwards, receiving mainly visual input from the image on the conical mirror.

Table 1

Predictive coding: weights of the lateral inhibition area with center pixel 0 and lateral pixels  $\pm 3$ ,  $\pm 2$ ,  $\pm 1$  (obtained from 2000 images recorded during typical trajectories of the robot)

Pixel	0	$\pm 1$	$\pm 2$	$\pm 3$
Weight	1.000	-0.510	0.003	0.007

The weighting function of the filter is formed by three input units ( $m = 3$ ) in either direction. Table 1 gives an average filter characteristic that was obtained from 2000 images recorded during typical trajectories of the robot. The visual stimuli were then temporally highpass filtered and amplified. Filtering as well as motion detection were the same as during simulation.

The transmission weights that couple the outputs of the large field integration units  $\beta_l$  and  $\beta_r$  to the motor system were the same as during simulation (Eq. (7)) and the control signals resulted from Eq. (10). The constant factors were set to  $k_f = 4.0$  mm/s and  $k_{or} = 4.0 \cdot 10^{-3}$  mm/s. Intrinsic noise signals with a Gaussian distribution (Fig. 12) caused random rotations around the vertical axis. The velocity of the motors could be set stepwise to  $\pm 8n$  mm/s with  $n = 1, \dots, 10$  for the left and right motor. The basic velocity was set to  $v_0 = 40$  mm/s, which was modulated by the visual motion signals. The robot was updated at a rate of 12 Hz.

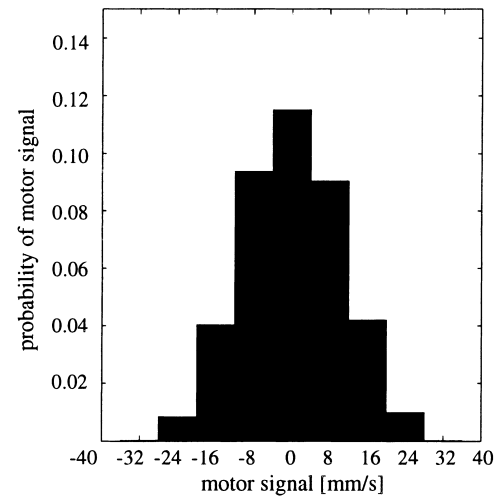


Fig. 12. Gaussian distribution of turning response due to the noise that is added to the motor signals.

## 5. Experiments with the robot

### 5.1. Optomotor response behavior

**Experiment 6.** In this situation, as in the fixation experiments with flies, the robot was only able to turn around its vertical axis within a circular arena (diameter: 45 cm). For the optomotor response a pattern with black and white stripes was painted onto the wall of the arena ( $\lambda = 51.4^\circ$ ). Instead of a constant rotatory bias of the drum, asymmetric motor signals were added to the left and right motor:  $\mp 24$  mm/s (this corresponds to  $\dot{\psi} = \pm 4.2^\circ/\text{frame}$ ).

**Result.** In the case of an asymmetric motor signal that led to a rotation of the robot about the vertical body-axis, the robot produced a compensatory turning response by the internally generated control signals compensating for 97% of the motor asymmetry (Fig. 13(a)).

### 5.2. Fixation behavior

**Experiment 7.** To test the fixation behavior, a single black stripe (angular width:  $25.7^\circ$ ) was painted onto the white wall of the arena. At the beginning of the experiment, the stripe was at an orientation of  $\psi = 57^\circ$  off the heading direction. Instead of measuring the

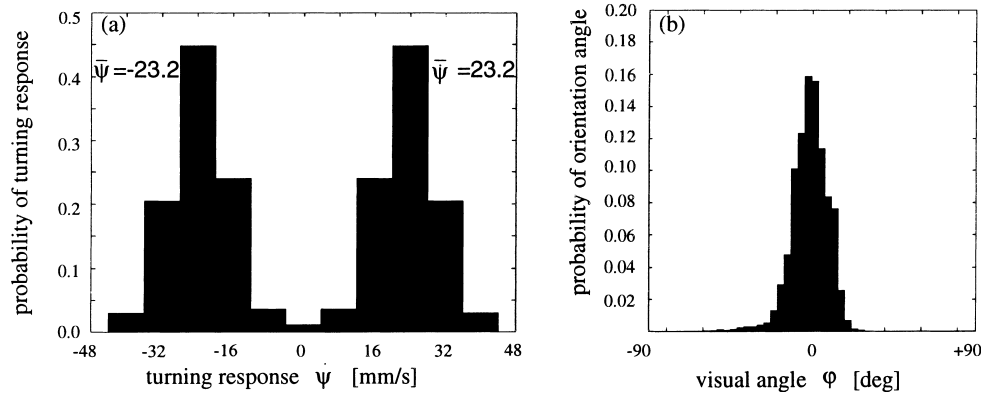


Fig. 13. (a) Histogram of the optomotor response in the presence of a motor asymmetry of the left and right motor ( $\mathbf{v}^a = (v_l^a, v_r^a) = (-24, +24)$  mm/s) (9700 steps). Compensatory motor signals of the left and right motor resulted in  $v_l = 23.2 \pm 7.2$  mm/s and  $v_r = -v_l$ . (b) Histogram (9700 steps) of the visual angle  $\varphi$  of the stripe's retinal image:  $\bar{\varphi} = -0.29^\circ \pm 10.36^\circ$ .

absolute orientation of the robot in the drum, we used the visual angle of the stripe's retinal image.

**Result.** In an arena with a single black stripe, the robot was able to orient itself towards the stripe after about 8 s and fixate on it (Fig. 13(b)). This was in accordance with the result from the simulation.

### 5.3. Approach behavior

**Experiment 8.** In the next experiment the robot was started from various positions and with various orientations in the arena (Fig. 14). The robot had two degrees of freedom: translation in the heading direction and rotation around the vertical axis. The rotatory and translatory velocities were set according to Eq. (5).

**Result.** When the robot had two degrees of freedom, i.e. was able to both translate and rotate, it approached the stripe in all tested cases (Fig. 14). The movement of the robot was guided by the motion perceived at the border of the stripe since no motion information can be derived from the uniform black stripe. Therefore, the agent often approached one border of the stripe instead of heading directly towards the middle of the stripe. The trajectories were obtained by a visual tracking system with a video camera recording the arena from a bird's-eye view. The system tracked a red marker on top of the robot.

## 6. Discussion

We have investigated whether one visuomotor controller is sufficient to generate both optomotor response and fixation behavior. We could in fact show that this was possible. Both the simulated agent and the *Khepera*<sup>TM</sup> robot showed optomotor response and fixation behavior depending on the particular environmental conditions. In addition the robot approached prominent objects in the arena if it was able to move around. In this section we discuss the sensorimotor control of the simulated agent and the robot and give suggestions for further improvements.

### 6.1. Visual system

The visual signals were spatially lowpass filtered in order to model the spatial sensor layout at the receptor layer. Predictive coding as suggested by Srinivasan et al. [34,45] together with temporal highpass filtering were applied in order to reduce redundant information from the image. The signal was then amplified such that it matched the full range of contrast sensitivity. The image processing procedure could be further improved because the spatial inhibitory surround that results from a filter designed with the predictive coding technique was slightly stronger than actually observed in the fly's lamina. More recent theories take another approach to extract the maximal possible spatiotemporal information for a given sensory system [47]. They

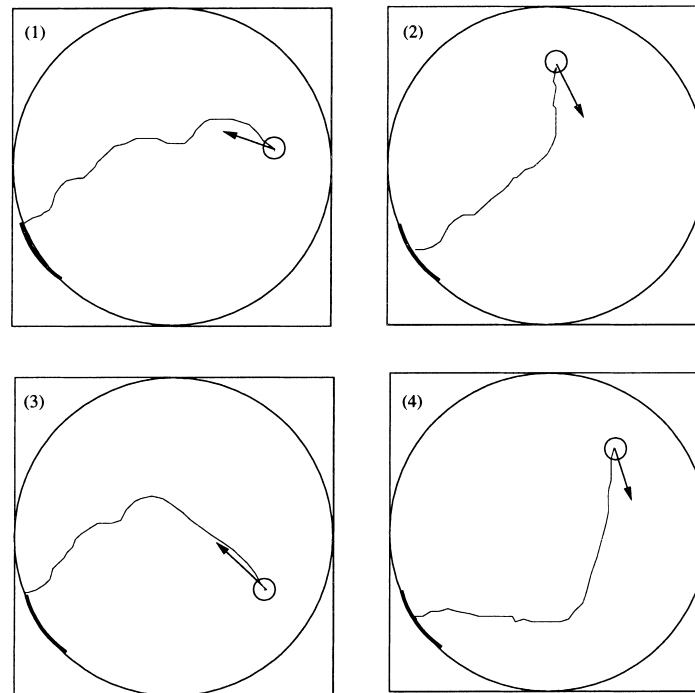


Fig. 14. Approach of single stripe in an arena. The robot starts with the orientations relative to the center point of the stripe  $\Delta\psi = -60^\circ, 60^\circ, 65^\circ,$  and  $70^\circ$ .

suggest a procedure to optimize a neural filter for an image sequence that the system normally encounters such that the information flow through the visual system is maximized. This may be implemented as a next step to model the lamina of flies in more detail. In addition, adaptive processes in the photoreceptors may be implemented to extend the range of luminances over which the sensors can operate. These processes will become essential if the system experiences large variations in lighting conditions, which was not the case in this study.

Missler and Kamangar [35] modeled the information processing of the fly's visual system for a tracking system. However, to design a controller that regulates the two behaviors of optomotor response and object fixation under real world conditions, some characteristics of the fly's visual system are essential which we included but which were missing in their model: (i) the reduction of signal redundancy in the lamina by lateral inhibition, (ii) the characteristic of the motion detectors that respond more strongly to progressive motion (from front to back) than to regressive motion

(from back to front), and (iii) the overlapping receptive fields as well as the sensitivity distribution of the tangential cells in the lobula plate.

## 6.2. Visuomotor control

Our work has demonstrated that with the controller the agents succeeded in both tasks of optomotor response and object fixation.

Experimental results on flies suggest a temporal integration stage of the output signals from the horizontal cells for the optomotor response [31,43]. We have shown that for our agent, integration of the image motion signals leads to an optomotor response behavior comparable to that of flies. Purely proportional control signals are not sufficient to compensate for the drum's rotation. Nevertheless, as in flies [39,49], no unstable behavior results due to the response characteristic of the motion detectors.

The following perceptual properties are essential to generate a fixation behavior similar to those in

flies: (i) an asymmetric response of the motion detectors to progressive and regressive motion, and (ii) the non-uniform spatial sensitivity function of the large field integration units with their overlapping fields in front of the agent.

### 6.2.1. Simulated agent

The fixation behavior of the simulated agent is comparable to that of flies. Similar to the transition of behavior in flies, the agent changed the fixation behavior from the fixation of the middle point between the stripes at  $\Delta\psi_s = 40^\circ$  to the fixation of the two single stripes for  $\Delta\psi_s \geq 60^\circ$ , where the agent fixates on either of the stripes for a certain amount of time. Analog to the findings in flies, for  $\Delta\psi_s = 60^\circ, 80^\circ$  and  $100^\circ$ , the estimated angular separation of the peaks of the histogram (Fig. 7(b)) was on an average smaller than the angular separation of the two stripes. When the agent fixated upon one of the two stripes, the motion signal that resulted from the second stripe in the lateral visual field produced a turning response in its direction. This behavior strongly depends on the non-uniform sensitivity function of the large field units and on the angular separation of the two stripes. For example, a uniform sensitivity distribution would cause a fixation on the center point between the two stripes. By the use of a threshold function for the outputs of the large field units, it may be possible to alter the agent's fixation behavior in the presence of two stripes. When fixating upon one stripe in the heading direction, the response to the second laterally placed stripe is smaller and could be reduced further by a threshold function. Like flies, the agent fixates on the center of the stripes for  $\Delta\psi_s = 180^\circ$ .

Differential equations have been used [37,42] to describe the optomotor response and fixation behaviors of flies under the same condition of one dynamic degree of freedom: rotation around the vertical axis. The phenomenological equation of motion describes in a first approximation the reaction of the fly under normal fixation by the instantaneous values of the pattern position and velocity (see also [38,41]). In contrast to our controller, the stages of image preprocessing, motion detection and processing of the visual motion information that lead to information about pattern position and velocity are not part of these simulations. Nevertheless, in the differential equation the shape of the distribution of the position-dependent term for

the one-stripe-fixation behavior is similar to the spatial sensitivity distribution  $S(j)$  of the large field units that integrate local motion information spatially in our model controller. Both indicate the attractiveness or the reaction strength towards the stripe located at a certain spatial position on the retina. In fact, the simulations of the two-stripe fixation behavior with differential equations and with our controller lead to comparable results.

### 6.2.2. Robot

The implementation of the control structure onto the robot was straightforward and the results showed that the simulations represent the real world conditions of the robot very well. We slightly changed the proportionality factor for the proportional and integral parts of the controller and reduced the time constant of the lowpass filter that simulated the transmission time through the controller. The robot was able to fixate on the black stripe and also to stabilize the retinal image by optomotor response. However, with two degrees of freedom the robot even approached prominent objects in the scene.

Our controller for the robot and the simulated agent is a simplification of the control structure of flies. One large simplification is that the robot is moving on a 2D plane. We do not model flying insects [22,48] but agents with two degrees of freedom: the rotation around the vertical body axis and the translation in the heading direction. The controller also does not take into account the fly's head movement relative to its body [20,32,48].

Other robots inspired by the visual motion processing of flies have been designed mainly for obstacle avoidance. Franceschini et al. [18] used a robot in a real environment that extracts the visual motion information from a ring sensor. Their robot has analog optoelectronic circuits on board to detect the local motion signals. The robot used the motion information for obstacle avoidance and a light sensor for the approach of a distant goal. The movements of the robot were piecewise linear translations with constant velocity and saccadic rotations, using the fact that during pure translations the image motion for objects in the distance is smaller than for objects close to the robot. Robots have been designed [51] for wall following in a corridor that execute translatory and rotatory movements at the same time. Again the translatory image

flow signals the distance to the walls. In order to obtain the translatory flow the number of rotations of the wheels are used to correct the image flow for rotatory motion. For optomotor response and object approach no pure translatory motion signal is necessary. Therefore, our robot executes rotations and translations at the same time with translatory and rotatory speed that varies according to the image motion, e.g., large progressive image motion reduces the forward speed.

## 7. Conclusion

We combined models of the visual information processing system in flies [21,27,28,34,45] with models of the control structure of their orientation behaviors [5,6,9,10,42,43] and transferred the simulations onto a robot that moves in a real environment. Testing the behavior of a robot in a real environment, we have been able to show that for optomotor response and object fixation, it is not necessary to implement separate modules for the two behaviors. One controller regulates both the optomotor response and the fixation of stationary objects. Which of the two behaviors predominates depends on the particular environment. The definition of a basic set of behaviors that enables the agent to accomplish a given task is a fundamental problem for the design of behavior-based architectures. The designer has to predict all possible interactions between behavioral modules and the environment. Thus the decomposition of the control architecture into behavioral modules has to be done very carefully.

Our results agree with results from previous simulations using differential equations [9,42,43] and experiments on flies (e.g., [5,42]) in that the large field cells alone are most probably not responsible for the full object fixation behavior. Full object fixation is mediated by other cells, as for example the small field cells [13], which respond selectively to motion in small areas of their receptive field, or to other position-induced mechanisms. This is especially the case for the tracking of moving objects, e.g., a male fly chasing another fly or a fly approaching a flower moving in the wind. The stabilizing role of the optomotor system does not allow for the fixation of moving targets against a featured background if fixation and optomotor system are coupled like in our controller [9,33,48,52]. Additional

sensorimotor control is necessary for full object fixation, e.g., in the presence of two and more objects (stripes) and especially in a non-stationary environment.

For further studies on autonomous robots and fly behavior, the implementation of our controller on an analog VLSI chip would be very useful. On such chips, motion detection mechanisms have been successfully developed [1,25,44]. These chips integrate both the photosensors and the motion computation on a single chip. As in biological systems, a parallel processing of visual signals is thus possible. These chips are very small and represent an alternative to conventional computer vision systems; however, there are still problems intrinsic to this approach. The sensors show a poor signal-to-noise ratio, and the performance decreases significantly at low contrast and low illumination levels. However, for the simulation of biological processes this does not have to be a disadvantage, as noise is intrinsic in all biological neural systems and is also an important feature, because it allows switching between behaviors which otherwise could get stuck in local minima.

## Acknowledgements

We would like to thank H. Krapp for many stimulating discussions on fly vision and fly behavior. We thank him and also A. Borst for helpful comments on preliminary versions of this paper.

## References

- [1] N. Ancona, T. Poggio, Optical flow from 1D correlation: application to a simple TTC detector, Memo no. 1375, AI Laboratory, MIT, Cambridge, MA, 1993.
- [2] R.D. Beer, *Intelligence as Adaptive Behavior*, Academic Press, San Diego, CA, 1990.
- [3] V. Braitenberg, *Vehicles — Experiments in Synthetic Psychology*, MIT Press, Cambridge, MA, 1984.
- [4] R.A. Brooks, A robust layered control system for a mobile robot, *IEEE Journal of Robotics and Automation* 2 (1) (1986) 14–23.
- [5] H. Bülthoff, *Drosophila* mutants disturbed in visual orientation: II. Mutants affected in movement and position computation, *Biological Cybernetics* 45 (1982) 71–77.
- [6] H.H. Bülthoff, T. Poggio, C. Wehrhahn, 3D analysis of the flight trajectory of flies *Drosophila melanogaster*, *Zeitschrift für Naturforschung* 35c (1980) 811–815.

- [7] R.H.S. Carpenter, *Movements in the Eyes*, Pion, London, 1979.
- [8] D.T. Cliff, Neural networks for visual tracking in an artificial fly, in: *Towards a Practice for Autonomous Systems: Proceedings of the First European Conference on Artificial Life*, MIT Press, Cambridge, MA, 1992, pp. 78–87.
- [9] T.S. Collett, Angular tracking and the optomotor response: An analysis of the visual reflex interaction in a hoverfly, *Journal of Comparative Physiology* 140 (1980) 145–158.
- [10] T.S. Collett, M.F. Land, Visual control of flight behavior in the hoverfly *Syrirta pipiens L.*, *Journal of Comparative Physiology* 99 (1975) 1–66.
- [11] H. Cruse, C. Bartling, G. Cymbalyk, J. Dean, M. Deifert, A modular artificial neural network for controlling a 6-legged walking system, *Biological Cybernetics* 72 (1995) 421–430.
- [12] A.P. Duchon, W.H. Warren, Robot navigation from a Gibsonian viewpoint, in: *Proceedings of the IEEE International Conference on Systems, Man and Cybernetics*, IEEE Press, Piscataway, NJ, 1994, pp. 2272–2277.
- [13] M. Egelhaaf, On the neural basis of figure-ground discrimination by relative motion in the visual system of the fly. I: Behavioral constraints imposed on the neural network and the role of the optomotor system, *Biological Cybernetics* 52 (1985) 123–140.
- [14] M. Egelhaaf, On the neural basis of figure-ground discrimination by relative motion in the visual system of the fly. II: Figure-detection cells, a new class of visual interneurons, *Biological Cybernetics* 52 (1985) 195–209.
- [15] M. Egelhaaf, On the neural basis of figure-ground discrimination by relative motion in the visual system of the fly. III: Possible input circuitries and behavioral significance of the FD-cells, *Biological Cybernetics* 52 (1985) 267–280.
- [16] M. Egelhaaf, A. Borst, W. Reichardt, Computational structure of a biological motion-detection system as revealed by local detector analysis in the fly's nervous system, *Journal of the Optical Society of America A* 6 (7) (1989) 1070–1087.
- [17] D. Floreano, F. Mondada, Automatic creation of an autonomous agent: Genetic evolution of a neural-network driven robot, in: *From Animals to Animats 3: Proceedings of the Third International Conference on Simulation of Adaptive Behavior*, MIT Press, Cambridge, MA, 1994, pp. 421–430.
- [18] N. Franceschini, J.M. Pichon, C. Blanes, From insect vision to robot vision, *Philosophical Transactions of the Royal Society of London B* 337 (1992) 283–294.
- [19] M.O. Franz, B. Schölkopf, M.A. Mallot, H.H. Bülthoff, Learning view graphs for robot navigation, *Autonomous Robots* 5 (1) (1998) 111–125.
- [20] G. Geiger, T. Poggio, On head and body movements of flying flies, *Biological Cybernetics* 25 (1977) 177–180.
- [21] K.G. Götz, Optomotorische Untersuchung des visuellen Systems einiger Augenmutanten der Fruchtfliege *Drosophila*, *Kybernetik* 2 (2) (1964) 77–92.
- [22] K.G. Götz, Flight control in *Drosophila* by visual perception of motion, *Kybernetik* 4 (1968) 199–208.
- [23] K.G. Götz, The optomotor equilibrium of the *Drosophila* navigation system, *Journal of Comparative Physiology* 99 (1975) 187–210.
- [24] K.G. Götz, H. Wenking, Visual control of locomotion in the walking fruitfly *Drosophila*, *Journal of Comparative Physiology* 85 (1973) 235–266.
- [25] R.R. Harrison, C. Koch, An analog VLSI model of the fly elementary motion detector, in: *Advances in Neural Information Processing Systems*, vol. 10, Morgan Kaufmann, San Mateo, CA, 1998, pp. 880–886.
- [26] I. Harvey, P. Husbands, D. Cliff, Seeing the light: Artificial evolution, real vision, in: *From Animals to Animats 3: Proceedings of the Third International Conference on Simulation of Adaptive Behavior*, MIT Press, Cambridge, MA, 1994, pp. 392–401.
- [27] B. Hassenstein, W. Reichardt, Systemtheoretische Analyse der Zeit-, Reihenfolgen- und Vorzeichenbewertung bei der Bewegungsperezeption des Rüsselkäfers *Chlorophanus*, *Zeitschrift für Naturforschung* 11b (1956) 513–524.
- [28] K. Hausen, Motion sensitive interneurons in the optomotor system of the fly, *Biological Cybernetics* 45 (1982) 143–156.
- [29] K. Hausen, Decoding of retinal image flow in insects, in: F.A. Miles, J. Wallman (Eds.), *Visual Motion and its Role in the Stabilization of Gaze*, Elsevier Science, Amsterdam, 1993, pp. 203–235.
- [30] K. Hausen, C. Wehrhahn, Neural circuits mediating visual flight control in flies. I. Quantitative comparison of neural and behavioral response characteristics, *Journal of Neuroscience* 9 (11) (1989) 3828–3836.
- [31] M. Heisenberg, R. Wolf, *Vision in Drosophila*, Springer, Berlin, 1984.
- [32] M.F. Land, Head movement of flies during visually guided flight, *Nature* 243 (1973) 299–300.
- [33] M.F. Land, T.S. Collett, Chasing behavior in houseflies *Fannia canicularis*, *Journal of Comparative Physiology* 89 (1974) 331–357.
- [34] S.B. Laughlin, Form and function in retinal processing, *Trends in Neurosciences* 10 (11) (1987) 478–483.
- [35] J.M. Missler, F.A. Kamangar, A neural network for pursuit tracking inspired by the fly visual system, *Neural Networks* 8 (3) (1995) 463–480.
- [36] F. Mondada, E. Franzi, P. Ienne, Mobile robot miniaturization: A tool for investigation in control algorithms, in: *Experimental Robotics III, Proceedings of the Third International Symposium on Experimental Robotics*, Springer, London, 1994.
- [37] M. Poggio, T. Poggio, Cooperative physics of fly swarms: An emergent behavior, AI Memo no. 1512, AI Laboratory, MIT, Cambridge, MA, 1994.
- [38] T. Poggio, W. Reichardt, A theory of the pattern induced flight orientation of the fly *Musca domestica*, *Kybernetik* 12 (1973) 185–203.
- [39] T. Poggio, W. Reichardt, Characterization of nonlinear interactions in the fly's visual system, in: W. Reichardt, T. Poggio (Eds.), *Theoretical Approaches in Neurobiology*, MIT Press, Cambridge, MA, 1981, pp. 64–84.
- [40] W. Reichardt, Autocorrelation, a principle for the evaluation of sensory information by the central nervous system, in: W.A. Rosenblith (Ed.), *Sensory Communication*, MIT Press/Wiley, New York, 1961, pp. 303–317.

- [41] W. Reichardt, T. Poggio, A theory of the pattern induced flight orientation of the fly *Musca domestica* II, *Biological Cybernetics* 18 (1975) 69–80.
- [42] W. Reichardt, T. Poggio, Visual control of orientation behavior in the fly. Part I: A quantitative analysis, *Quarterly Reviews of Biophysics* 9 (3) (1976) 311–375.
- [43] W. Reichardt, T. Poggio, K. Hausen, Figure-ground discrimination by relative movement in the visual system of the fly. Part II: Towards the neural circuitry 1, *Biological Cybernetics* 46 (Suppl.) (1983) 1–30.
- [44] R. Sarpeshkar, J. Kramer, G. Indiveri, C. Koch, Analog VLSI architectures for motion processing: from fundamental limits to system applications, *Proceedings of IEEE* 84 (7) (1996) 969–982.
- [45] M.V. Srinivasan, S.B. Laughlin, A. Dubs, Predictive coding: A fresh view of inhibition in the retina, *Proceedings of the Royal Society of London B* 216 (1982) 427–459.
- [46] N. Tinbergen, *Instinktlehre — vergleichende Erforschung angeborenen Verhaltens*, Parey Verlag, Berlin, 1953.
- [47] J.H. van Hateren, Theoretical predictions of spatiotemporal receptive fields of fly LMCs, and experimental validation, *Journal of Comparative Physiology A* 171 (1992) 157–170.
- [48] H. Wagner, Flight performance and visual control of flight of the free-flying housefly (*Musca domestica* L.), III. Interactions between angular movement induced by wide- and smallfield stimuli, *Philosophical Transactions of the Royal Society of London B* 312 (1986) 581–595.
- [49] A.-K. Warzecha, M. Egelhaaf, Intrinsic properties of biological motion detectors prevent the optomotor control system from getting unstable, *Philosophical Transactions of the Royal Society of London B* 351 (1996) 1579–1591.
- [50] B. Webb, Using robots to model animals: a cricket test, *Robotics and Autonomous Systems* 16 (1995) 117–134.
- [51] K. Weber, S. Venkatesh, M.V. Srinivasan, Insect inspired behaviours for the autonomous control of mobile robots, in: M.V. Srinivasan, S. Venkatesh (Eds.), *From Living Eyes to Seeing Machines*, Oxford University Press, Oxford, 1997.
- [52] C. Wehrhahn, T. Poggio, H.H. Bülthoff, Tracking and chasing in houseflies (*Musca*), *Biological Cybernetics* 45 (1982) 123–130.
- [53] R.C. Gonzales, R.E. Woods, *Digital Image Processing*, Addison-Wesley, Reading, MA, 1992.



**Susanne A. Huber** is currently a research fellow at the Department of Psychology, University of Zurich, Switzerland. In 1993 she received a Diploma in Physics from the Eberhard-Karls-University in Tübingen, Germany. She holds a Ph.D. Degree in the Natural Sciences from the Eberhard-Karls-Universität in Tübingen. From 1993 to 1997 she worked as a research scientist at the Max-Planck-Institute

for Biological Cybernetics in Tübingen. Since 1998 she works at the General and Developmental Psychology Group at the University of Zurich. Her research interests include behavior-based robotics as well as children's development of skilled behavior and knowledge about the physical world.



**Matthias O. Franz** graduated with a M.Sc. in Atmospheric Sciences from SUNY at Stony Brook, NY, in 1994. In 1995, he received a Diploma in Physics from the Eberhard-Karls-Universität, Tübingen, Germany, where he also finished his Ph.D. in Computer Science in 1998. His thesis research on minimalistic visual navigation strategies was done at the Max-Planck-Institut für biologische Kybernetik, Tübingen. He is currently working as a researcher at DaimlerChrysler Research & Technology, Ulm, Germany. His scientific interests include optic flow, autonomous navigation, and natural image statistics.



**Heinrich Bülthoff** is scientific member of the Max-Planck-Gesellschaft and Director at the Max-Planck-Institute for Biological Cybernetics in Tübingen. He directs a group of about 35 biologists, computer scientists, mathematicians, physicists and psychologists working on psychophysical and computational aspects of higher-level processes in the following area: object and face recognition, sensory-motor integration, spatial cognition, autonomous navigation and artificial life, computer graphics psychophysics, and perception and behavior in virtual environments. Professor Bülthoff is involved in many international collaborations on these topics and is a member of the following scientific societies: Psychonomics Society since 1996, Computer Society of the IEEE since 1988, Society of Neuroscience since 1987, Association for Research in Vision and Ophthalmology since 1984. He holds a Ph.D. degree in the Natural Sciences from the Eberhard-Karls-Universität in Tübingen. From 1980 to 1985 he worked as a research scientist at the Max-Planck-Institute for Biological Cybernetics in Tübingen. He then moved to the USA to work at the Massachusetts Institute of Technology in Cambridge and later became Professor at Brown University in Providence. After he had returned to the Max-Planck-Institute in 1993, he became an Honorary Professor at the Eberhard-Karls-Universität in 1996.